

Matrix Isolation of Germacyclopentadienes: Direct Spectroscopic Evidence for Germylene-to-Germene Photochemical Interconversion

Valery N. Khabashesku,^{*,1a-c} Sergei E. Boganov,^{1a} Dean Antic,^{1b}
Oleg M. Nefedov,^{1a} and Josef Michl^{*,1b,c}

Zelinsky Institute of Organic Chemistry, Russian Academy of Sciences, 47 Leninsky prospekt,
Moscow 117913, Russian Federation, and Department of Chemistry,
University of Colorado at Boulder, Boulder, Colorado 80309-0215

Received May 16, 1996[®]

UV irradiation of matrix-isolated 1,1-diazo-1-germacyclopent-3-ene (**4b**) produced 1*H*-germole (1-germacyclopenta-2,4-diene; **1b**) and 1-germacyclopent-3-ene-1,1-diyl (**2b**) as major products along with 3*H*-germole (1-germacyclopenta-1,4-diene; **5b**) and 2*H*-germole (1-germacyclopenta-1,3-diene; **6b**) as minor products. During irradiation at selected wavelengths a photoconversion of **1b** into **5b** and reversible interconversion of **2b** and **6b** have been observed and provide experimental evidence for a germylene-to-germene rearrangement. Similar experiments were carried out on deuterated analogues, and the precursor **4b-d₆** produced **1b-d₆**, **2b-d₆**, **5b-d₆**, and **6b-d₆**. Full vibrational assignment in the IR spectra of **1b**, **2b**, **5b**, and **6b** has been proposed on the basis of restricted Hartree–Fock (DZ+d) calculations for those molecules and their *d₆* analogues and literature data on the silicon analogues **1a**, **2a**, **5a**, **6a**, and other related molecules. The UV–vis spectra are interpreted by comparison with the experimental and computed transition energies of the silacyclopentadiene isomers **1a**, **2a**, **5a**, and **6a**. The Ge=C stretching frequencies are low and provide evidence for C=Ge–C=C and Ge=C–C=C π conjugation, which is somewhat weaker than that established earlier in the silacyclopentadienes **5a** and **6a**.

Introduction

The five-membered group 14 (Si, Ge, Sn) metallacyclic dienes (metalloles) have attracted the attention of organometallic chemists for the last 50 years due to their high reactivity both as neutral molecules and transition-metal complexes and as ionic species.^{2,3} It is well established that C-substituted metalloles are stable as monomers under ambient conditions and are relatively easy to prepare. In contrast, C-unsubstituted metalloles are kinetically unstable toward Diels–Alder type dimerization, and only a few members of this family of compounds have been identified as monomers.⁴ The parent compounds, 1*H*-metalloles (**1**), are even more reactive and have been postulated as transient species. Only recently, a UV and IR spectroscopic characterization of 1*H*-silole (**1a**) by matrix isolation⁵ as well as an MS determination⁶ of its gas-phase ionization potential were reported. To our knowledge,

parent 1*H*-metalloles containing a group 14 metal atom heavier than silicon have not yet been directly characterized.

In previous studies^{5,6} the parent silole **1a** was efficiently accessed from precursors for 1,1-silacyclopent-3-ene-1,1-diyl (**2a**). It was produced in the gas phase by vacuum pyrolysis of 5-silaspiro[4.4]nona-2,7-diene (**3a**) and of 1,1-diazo-1-silacyclopent-3-ene (**4a**) and in a solid matrix by irradiation of matrix-isolated **4a**. Inspired by these results, we decided to carry out a matrix isolation study of the decomposition reactions of potential precursors for the germanium analogue of **2a**, the cyclic germylene **2b**, in expectation of the ultimate production of 1*H*-germole (**1b**) by analogy with the known thermal or photochemical isomerization of the silylene **2a** into 1*H*-silole **1a** via consecutive hydrogen shifts. The choice of the germanium analogues of **3a** and **4a**, 5-germaspiro[4.4]nona-2,7-diene (**3b**) and 1,1-diazo-1-germacyclopent-3-ene (**4b**), as precursors for the germylene **2b** seemed obvious. However, it was found in previous matrix work⁷ that the 3,4-dimethyl derivative of the germylene **2b** is thermally unstable under the conditions of vacuum pyrolysis (10⁻⁴ Torr, 700 °C) of its precursors, 2,3-dimethyl or 2,3,7,8-tetramethyl derivatives of **3b**, even though it could be chemically

[®] Abstract published in *Advance ACS Abstracts*, October 1, 1996.

(1) (a) Zelinsky Institute of Organic Chemistry. Present address: Department of Chemistry, Rice University, Houston, TX 77251-1892. (b) University of Colorado at Boulder. (c) Part of the work was done during the stay of V.N.K. and J.M. at the University of Texas at Austin.

(2) Dubac, J.; Laporterie, A.; Manuel, G. *Chem. Rev.* **1990**, *90*, 215. (3) Colomer, E.; Corriu, R. J. P.; Lheureux, M. *Chem. Rev.* **1990**, *90*, 264.

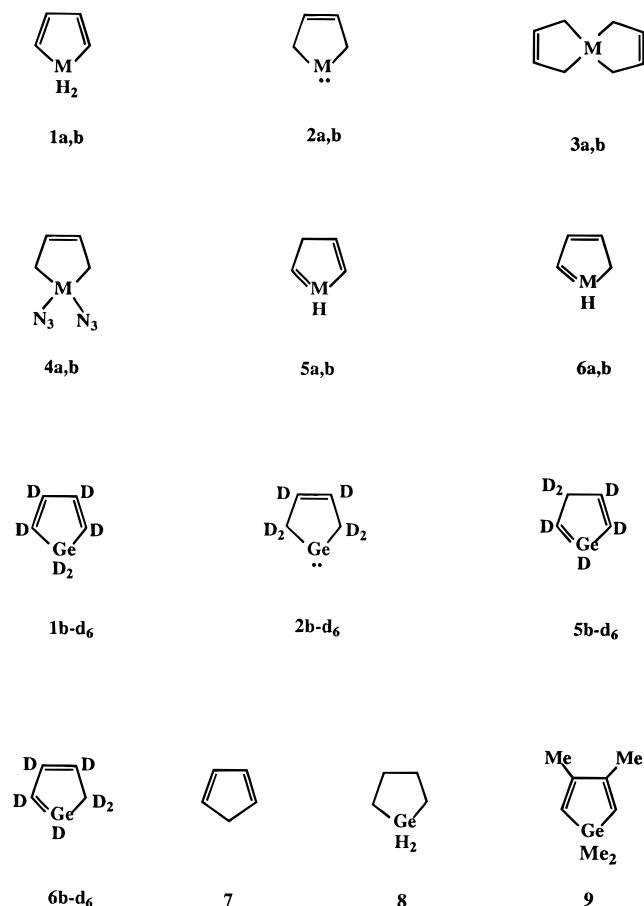
(4) 1,1-Dimethylsilole: (a) Laporterie, A.; Mazerolles, P.; Dubac, J.; Illoughmane, H. *J. Organomet. Chem.* **1981**, *206*, C25. (b) Laporterie, A.; Dubac, J.; Mazerolles, P.; Illoughmane, H.; *J. Organomet. Chem.* **1981**, *216*, 321. (c) Burns, G. T.; Barton, T. J. *J. Organomet. Chem.* **1981**, *209*, C25. 1,1-Dimethylgermole: (d) Laporterie, A.; Manuel, G.; Dubac, J.; Mazerolles, P.; Illoughmane, H. *J. Organomet. Chem.* **1981**, *210*, C33. (e) Laporterie, A.; Illoughmane, H.; Dubac, J. *J. Organomet. Chem.* **1983**, *244*, C12. (f) Guimon, C.; Pfister-Guillouzo, G.; Dubac, J.; Laporterie, A.; Manuel, G.; Illoughmane, H. *Organometallics* **1985**, *4*, 636. 1,1-Dibutylstannole: (g) Ashe, A. J., III; Mahmoud, S. *Organometallics* **1988**, *7*, 1878.

(5) (a) Khabashesku, V. N.; Balaji, V.; Boganov, S. E.; Matveichev, P. M.; Chernyshev, E. A.; Nefedov, O. M.; Michl, J. *Mendeleev Commun.* **1992**, 38. (b) Khabashesku, V. N.; Balaji, V.; Antic, D.; Boganov, S. E.; Nefedov, O. M.; Michl, J. XXVth Silicon Symposium, Indianapolis, IN, March 26–27, 1993; Indiana Univ.–Purdue Univ.: Indianapolis, IN, 1993; Abstracts, p D-11. (c) Khabashesku, V. N.; Balaji, V.; Boganov, S. E.; Nefedov, O. M.; Michl, J. *J. Am. Chem. Soc.* **1994**, *116*, 320.

(6) Khabashesku, V. N.; Boganov, S. E.; Faustov, V. I.; Gomory, A.; Besenyei, I.; Tamas, J.; Nefedov, O. M. *High Temp. Mater. Sci.* **1995**, *33*, 125.

(7) Mazerolles, P.; Khabashesku, V. N.; Boganov, S. E.; Nefedov, O. M. *Bull. Acad. Sci. USSR, Div. Chem. Sci. (Engl. Transl.)* **1989**, 1428.

Chart 1



trapped by butadiene during their flow pyrolysis (1–10 Torr) at lower temperatures (~400 °C). On the basis of those results, we did not attempt to perform vacuum pyrolysis of the precursors **3b** and **4b** and chose the photochemical decomposition of the diazide **4b** as a route to the germylene **2b**. This choice has precedent in the previous use of group 14 organometallic geminal diazides for matrix *in situ* photogeneration of dimethylsilylene,^{8c} dimethylgermylene,⁹ and the cyclic silylene **2a**.⁵

In the present paper we provide a full report on UV–vis and FTIR spectroscopic characterization of the germylene **2b** and the isomeric germacyclopentadienes (1*H*-, 2*H*- and 3*H*-metalloles) **1b**, **5b**, and **6b**, as well as the deuterated analogues **1b-d₆**, **2b-d₆**, **5b-d₆**, and **6b-d₆**. Some of these results were previously reported at conferences.^{5b,10}

Experimental Section

General Methods. ¹H and ¹³C NMR spectra of **4b** and **4b-d₆** were recorded on JEOL FX90Q and Bruker AM300 spec-

(8) (a) Reisenauer, H. P.; Mihm, G.; Maier, G. *Angew. Chem.* **1982**, *94*, 864. (b) Maier, G.; Mihm, G.; Reisenauer, H. P.; Littman, D. *Chem. Ber.* **1984**, *117*, 2369. (c) Raabe, G.; Vancik, H.; West, R.; Michl, J. *J. Am. Chem. Soc.* **1986**, *108*, 671. (d) Maier, G.; Reisenauer, H. P.; Schoettler, K.; Wessolek-Kraus, U. J. *J. Organomet. Chem.* **1989**, *366*, 25.

(9) Barrau, J.; Bean, D. L.; Welsh, K. M.; West, R.; Michl, J. *Organometallics* **1989**, *8*, 2606.

(10) (a) Khabashesku, V. N.; Bogdanov, S. E.; Antic, D.; Michl, J.; Nefedov, O. M. The Fifth Conference on Carbene Chemistry (with International Participation), Sept 16–18, 1992, Moscow, Russia; Russian Acad. Sci. at Book Palace, Inc.: Moscow, Russia, 1992; Abstracts, pp 157–158. (b) Khabashesku, V. N.; Nefedov, O. M. International Conference on Low-Temperature Chemistry, Sept 5–9, 1994, Moscow, Russia; M. V. Lomonosov State Univ.: Moscow, Russia, 1994; Abstracts, p 24.

trometers. Mass spectral analysis was performed on a Varian MAT 311A instrument (ionization energy 70 eV, direct inlet probe). Butadiene-*d*₆ was purchased from MSD Isotopes.

1,1-Diazido-1-germacyclopent-3-ene (4b). NaN₃ (1 g, 15.4 mmol) was added under an Ar atmosphere to 1,1-dichloro-1-germacyclopent-3-ene (1 g, 5.1 mmol) in dry acetonitrile (10 mL, prepared in 60% yield from the dioxane complex of dichlorogermylene¹¹ and butadiene¹²). The mixture was stirred for 4 h at 40 °C, cooled to room temperature, dry diethyl ether (8 mL) was added, the precipitate was filtered off, the solvent was evaporated, and **4b** was isolated by bulb-to-bulb distillation (60–70 °C/0.1 Torr) into a liquid-nitrogen-cooled trap. Yield: 0.4 g (40%). ¹H NMR (C₆D₆, 90 MHz): δ 1.32 s (4H), 5.58 s (2H). ¹H NMR (CDCl₃, 300 MHz): δ 1.94 s, 6.14 s. ¹³C{¹H} NMR (C₆D₆, 90 MHz): δ 16.29 (CH₂), 128.81 (=CH). ¹³C{¹H} NMR (CDCl₃, 300 MHz): δ 16.99, 129.03. IR (Ar matrix, 11 K): 3045 (w), 3040 (w), 2954 (vw), 2921 (vw), 2554 (vw), 2538 (vw), 2130 (vvs), 2110 (vvs), 1610 (m), 1410 (w), 1390 (w), 1366 (w), 1340 (vw), 1277 (vs), 1269 (vs), 1210 (w), 1170 (w), 1156 (w), 1104 (s), 1098 (m), 948 (m), 788 (w), 684 (m), 679 (m), 659 (w), 640 (s), 579 (w), 559 (w), 505 (w), 492 (s), 485 (s) cm⁻¹. UV (3-methylpentane): λ_{max} 243 nm (ε = 80). EIMS: *m/z* (relative intensity) (given for ⁷³Ge) 211(2), 169 (9), 142 (38), 127 (19), 126 (19), 115 (66), 87 (13), 54 (100). HRMS: *m/z* (calcd for C₄H₆⁷²GeN₆ 210.9908) 210.9908; (calcd for C₄H₆⁷⁰GeN₆ 208.9929) 208.9924.

1,1-Diazido-1-germacyclopent-3-ene-d₆ (4b-d₆) was prepared in 50% yield as described above for **4b**. 1,1-Dichloro-1-germacyclopent-3-ene-*d*₆ was prepared in 53% yield from dioxane–dichlorogermylene complex and butadiene-*d*₆.¹² It was identified by GC (5% SE 30 packed column) comparison with the undeuterated sample and by its ¹³C{¹H} NMR spectrum (CDCl₃, 300 MHz): δ 128.41 t (=CD), 24.82 p (=CD₂). **4b-d₆**: ¹³C{¹H} NMR (CDCl₃) δ 128.4 t (=CD), 16.05 p (CD₂); ¹³C{¹H} NMR (C₆D₆) δ 15.7 p (CD₂), the signals of CD groups overlapped with those of solvent; IR (Ar matrix, 11 K) 2538 (vw), 2284 (w), 2276 (w) 2220 (vw), 2130 (vs), 2110 (vs), 1578 (m), 1281 (s), 1269 (s), 1215 (w), 1167 (m), 1129 (w), 1062 (m), 1034 (m), 1004 (w), 877 (w), 843 (m), 831 (w), 773 (m), 763 (m), 685 (m), 628 (m), 525 (m), 486 (s) cm⁻¹; HRMS *m/z* (calcd for C₄D₆⁷⁴GeN₆ 218.02432) 218.02438.

Matrix Isolation Spectroscopy. A highly diluted vapor of diazide **4b** or **4b-d₆**, obtained by passing argon over liquid **4b** or **4b-d₆** kept at 5 °C, was deposited on a CsI or sapphire window cooled to 26–28 K with an Air Products CSA-202 Displex closed-cycle helium cryostat, and the temperature was lowered to 11 K for irradiation and spectral measurements. The shroud of the cryostat was equipped with outer CsI and/or Suprasil windows. Experiments in a 3-methylpentane (3-MP) glass at 77 K were performed in a 5 × 2 × 0.5 cm Suprasil cell suspended in a liquid-nitrogen-filled quartz Dewar fitted with Suprasil windows.

The diazides **4b** and **4b-d₆** were irradiated with a low-pressure mercury lamp (254 nm) or a Lambda Physik EMG 50 excimer laser (KrF, 248 nm). Complete photodestruction of **4b** or **4b-d₆** took 2–5 h with the lamp and 1–2.5 h with the laser, depending on the thickness of the matrix. Photobleaching experiments on the primary photolysis products were done with the 308 nm XeCl excimer laser, a 454 nm Ar ion laser, or a 1000 W high-pressure mercury–xenon lamp equipped with cutoff or broad-band filters. UV–vis spectra were recorded on a Cary 17D spectrophotometer interfaced to a PDP-11/23 computer. IR spectra were taken in the 400–4000 cm⁻¹ spectral range on a Nicolet 6000 series FTIR spectrometer with 1 cm⁻¹ resolution (500 scans), using a liquid-nitrogen-cooled MCT detector.

Calculations. Optimized *ab initio* geometries of **1b**, **2b**, **5b**, and **6b** and vibrational frequencies and intensities for

(11) Nefedov, O. M.; Kolesnikov, S. P.; Ioffe, A. I. *Izv. Akad. Nauk SSSR, Ser. Khim.* **1976**, 619.

(12) Kolesnikov, S. P.; Rogozhin, I. S.; Nefedov, O. M. *Izv. Akad. Nauk SSSR, Ser. Khim.* **1974**, 2379.

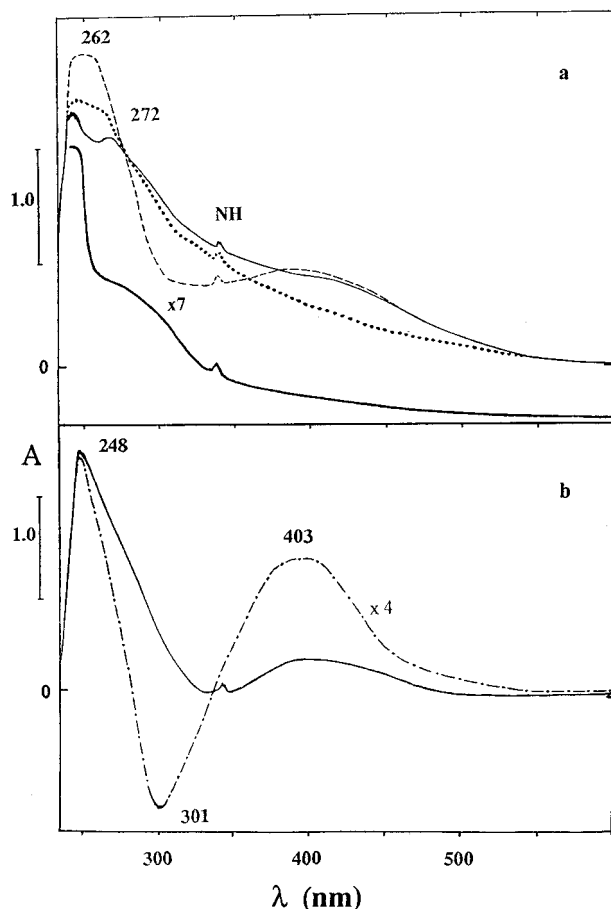


Figure 1. UV-vis spectra (Ar, 12 K): (a) 248 nm photolysis products from **4a**^{5c} (fat solid line, displaced vertically for clarity and shifted down by 0.5) and 248 nm photolysis products from **4b** before (solid line) and after (dashed line) bleaching by 308 nm light, followed by further irradiation with 454 or 254 nm light (dotted line); (b) spectra after further bleaching by 308 nm light (solid line) and after taking the difference (dash-dotted line) of the latter spectrum (positive) and that shown by the dotted line in Figure 1a (negative).

these molecules and their *d*₆ analogues were computed at the Hartree-Fock SCF level using a DZ+d basis set for germanium,¹³ carbon, and hydrogen.¹⁴ The frequencies were calculated using the analytical second-derivative method and harmonic approximation and were uniformly scaled by 90% before comparison with experimental data. All calculations were carried out using the GAUSSIAN 90 program¹⁵ running on an IBM RS-6000-550 computer, and their results are collected in Tables 1–9.

Results

The UV-vis spectrum of the light yellow matrix resulting from 248 nm irradiation of matrix-isolated **4b** (Figure 1a) contains a band at 248 nm, a broad band at 260–320 nm peaking near 272 nm, a sharp peak at 337 nm due to NH molecules formed from traces of HN₃ and disregarded in the following, and a weak absorption

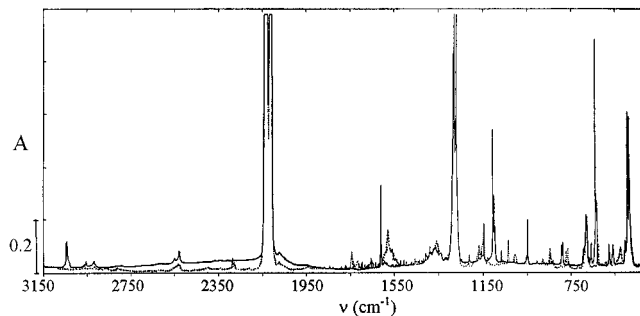


Figure 2. IR spectra (Ar, 12 K) of diazides **4b** (solid line) and **4b-d**₆ (dotted line).

band at 370–460 nm. This spectrum is quite similar to that obtained after the irradiation of the matrix-isolated silicon analog **4a**, which also shows a broad band at 260–350 nm with a maximum centered at 278 nm (Figure 1a).⁵ This latter band was attributed to the silole **1a**.

A comparison of the known wavelengths of UV absorption maxima of stable 1,1,3,4-tetramethylgermole and 1,1,3,4-tetramethylsilole shows a slightly lower value for the former (280 nm¹⁶) than the latter (285 nm²), suggesting that the UV absorption maximum for transient germole **1b** will be at slightly shorter wavelengths than that of silole **1a** (278 nm⁵). The best candidate for this assignment is the band at 272 nm (264 nm in a 3-MP matrix at 77 K). The other two bands present in this spectrum belong to another photoproduct, since they simultaneously disappear during further irradiation with 254 nm or visible (454 nm) light, while the band at 272 nm remains.

This preliminary assignment of the UV band at 272 nm to germole **1b** is supported by the IR spectrum of the matrix. The IR peaks of **4b** gradually disappear during the irradiation with 248 or 254 nm light until the decomposition of **4b** is complete. This is best followed by monitoring the bands in the 2000–2200 cm⁻¹ region, where two very intense peaks of **4b** at 2210 and 2130 cm⁻¹ (Figure 2) are ultimately replaced by a strong band at 2096 cm⁻¹ with a shoulder at 2015 cm⁻¹, and by two medium-intensity bands at 2115 and 2127 cm⁻¹ (Figure 3b). In the IR spectrum of the photoproducts from **4b-d**₆ (inset in Figure 3b) these bands were not found, indicating the absence of a monoazide, such as an azidogermanimine. Instead, several new bands are observed in the 1450–1650 cm⁻¹ region.

The Ge–H stretching vibration bands in the IR spectra of tetra-*C*-phenyl-1*H*-germoles¹⁷ are found between 2040 and 2060 cm⁻¹, and in Ar matrix-isolated **1b** those bands are expected to lie 30–40 cm⁻¹ higher, as was the case for **1a** when compared with the tetra-*C*-phenyl- or tetra-*C*-methyl-substituted 1*H*-siloles.² This would be compatible with an assignment of the band at 2096 cm⁻¹ (with a shoulder at 2015 cm⁻¹) to one of the Ge(sp³)–H stretches in **1b**. Additional support for this assignment is provided by the observation of a medium-strong band at 1522 cm⁻¹ in the IR spectrum of 248 nm photolysis products of **4b-d**₆.

(13) (a) Nagase, S.; Kudo, T. *Organometallics* **1984**, *3*, 324. (b) Olbrich, G. *Chem. Phys. Lett.* **1980**, *73*, 110.

(14) Dunning, T. H. *J. Chem. Phys.* **1970**, *53*, 2823.

(15) Frisch, M. J.; Head-Gordon, M.; Trucks, G. W.; Foresman, J. B.; Schlegel, H. B.; Raghavachari, K.; Robb, M.; Binkley, J. S.; Gonzalez, C.; Defrees, D. J.; Fox, D. J.; Whiteside, R. A.; Seeger, R.; Melius, C. F.; Baker, J.; Martin, R. L.; Kahn, L. R.; Stewart, J. J. P.; Topiol, S.; Pople, J. A. *Gaussian 90*; Carnegie-Mellon Quantum Chemistry Publishing Unit: Pittsburgh, PA, 1990.

(16) Dubac, J.; Laporterie, A.; loughmane, H. *J. Organomet. Chem.* **1985**, *293*, 295.

(17) Curtis, M. D. *J. Am. Chem. Soc.* **1967**, *89*, 4241.

(18) (a) Kudo, T.; Nagase, S. *Chem. Phys. Lett.* **1981**, *84*, 375. (b) Trinquier, G.; Barthelat, J.-C.; Satgé, J. *J. Am. Chem. Soc.* **1982**, *104*, 5931.

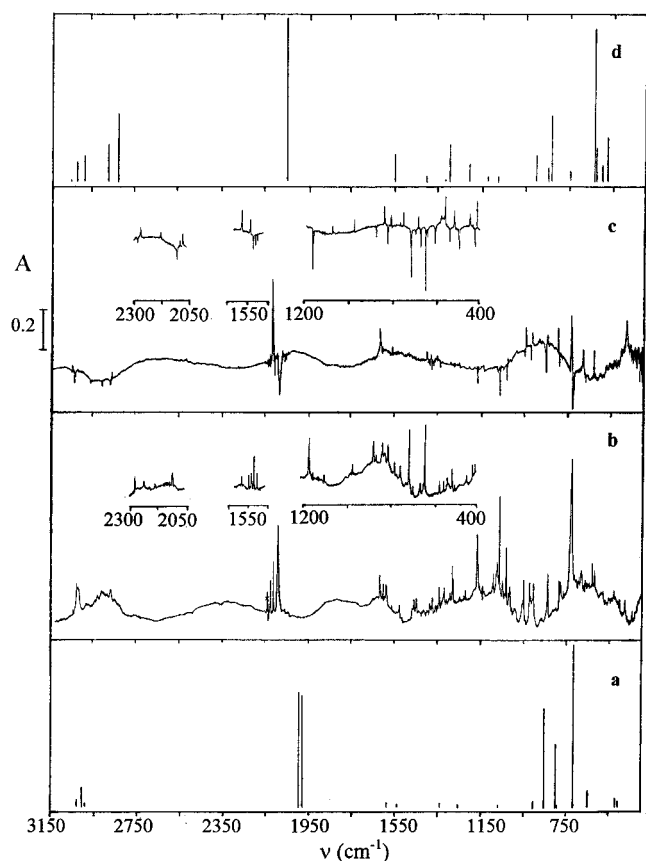


Figure 3. IR spectra (Ar, 12 K): (a) **1b**, calculated; (b) products of 248 nm irradiation of **4b** ($x = \text{HN}_3$) and **4b-d₆** (inset); (c) difference of the spectrum shown under (b) before (negative) and after (positive) further 308 nm irradiation (deuterated species in inset); (d) **5b**, calculated.

The assignment of all the other IR bands in the spectra shown in Figure 3b is based on the observation of their differential behavior in photobleaching experiments and on comparison with the spectra calculated for **1b**, **2b**, **5b**, **6b**, and their d_6 analogues. Bleaching the matrix produced by the initial 248 nm irradiation (solid line in Figure 1a) with 308 nm light produces a new band at 262 nm and causes an increase in the 370–460 nm band. This clearly indicates the presence of two or more photoproducts in the resulting matrix (dashed line in Figure 1a). In the difference FTIR spectrum, shown in Figure 3c, the IR bands of the products of the 308 nm irradiation are shown by positive peaks and bands of the species destroyed by the 308 nm irradiation are shown by negative peaks. Comparison with the calculated spectrum suggests that the negative peaks belong to **1b** (Figure 3a). For instance, in the 2000–2200 cm^{-1} spectral region, one band out of the three observed before bleaching (Figure 3b) corresponds to the most intense positive peak at 2127 cm^{-1} in Figure 3c, while the two others, one at 2115 cm^{-1} , whose origin is discussed below, and one at 2096 cm^{-1} (with a shoulder at 2099 cm^{-1}), already tentatively attributed to **1b**, appear as negative peaks. The positive peak at 2127 cm^{-1} is associated with the product that absorbs at 262 nm, since it is not affected when visible light is used to destroy the species that absorbs at 370–460 nm.

On the basis of the evidence discussed so far, we propose that **1b** is a major constituent of the matrix produced by initial 248 nm or 254 nm irradiation and that it is characterized by a UV peak at 272 nm and a

series of IR peaks shown negative in Figure 3c. Next, we need to identify the products of its photodestruction with 308 nm light. Reference to the silicon analogue is again helpful. After irradiation with 308 nm light, **1a** undergoes a 1,3-H shift into 3*H*-silole **5a**,⁵ which has a UV absorption peak at 270 nm. Therefore, we believe that the most likely assignment of the 262 nm photoproduct from 308 nm irradiation of **1b**, which has a strong IR peak at 2127 cm^{-1} , is to 3*H*-germole (1-germacyclopent-1,4-diene) **5b**. This assignment is supported by the calculated IR spectrum of **5b** (Figure 3d), which predicts a higher frequency for its $\text{Ge}(\text{sp}^2)\text{-H}$ stretch than for the $\text{Ge}(\text{sp}^3)\text{-H}$ stretching modes in germole **1b** (Figure 3a), in analogy to the difference between **5a** and **1a**.⁵ In the difference spectrum obtained with the perdeuterated starting material (inset in Figure 3c), the 2127 cm^{-1} peak is shifted to the 1450–1650 cm^{-1} spectral region. In accordance with calculations, we associate the $\text{Ge}(\text{sp}^2)\text{-D}$ stretch in photoproduct **5b-d₆** with a positive peak at 1547 cm^{-1} .

The second photoproduct from the 308 nm irradiation, characterized by a broad 370–460 nm absorption band (Figure 1a, dashed line), is tentatively assigned to the germylene **2b**. This is the only reasonable structure for which visible absorption would be expected, and the analogy to the silylene **2a**^{5c} is again obvious. This assignment agrees with the results of further bleaching experiments on the matrix. Irradiation with 454 nm light, only absorbed by this product, but also with 254 nm light, bleaches it (dotted line in Figure 1a). Further irradiation of the matrix with 308 nm light restores the 370–460 nm band and causes the UV–vis spectrum to take the appearance shown in Figure 1b by a full line. The spectra of the products formed during these successive irradiation experiments can be separated by consideration of the difference spectra. The difference UV–vis spectrum shown in Figure 1b by a dash-dotted line shows the spectrum indicated by a full line in Figure 1a minus the spectrum shown by a dotted line in Figure 1b. The corresponding difference FTIR spectrum, obtained for the same matrices, is presented in Figure 4b. The difference UV–vis spectrum shows two positive bands, at 248 and 370–460 nm, and a negative band at 301 nm. The band at 301 nm is particularly difficult to detect in the initial spectrum of photolysis products of **4b** (Figure 1a, full line), since it is overlapped by strong absorption of the main photoproduct, **1b**. The bands at 248 and 370–460 nm are changing simultaneously, in proportion, when the matrix is irradiated with either 254 or 454 nm light, proving that they both belong to the same single species. This species is characterized by the IR spectrum shown in Figure 4b by positive peaks, while the species responsible for the 301 nm band is associated with the negative peaks. Note that 454 nm irradiation of the 370–460 nm species also produces a small amount of **1b**, as evidenced by the negative peak at 2096 cm^{-1} in the difference spectrum shown in Figure 4b.

A preliminary assignment of the 370–460 nm absorption band to **2b** has already been made above, but the latter photobleaching observations proved that not only this band but also a band at 248 nm should be attributed to **2b**. That conclusion is supported by the already established⁴ fact that the silicon analog of **2b**, the silylene **2a**, also shows two bands in the UV–vis

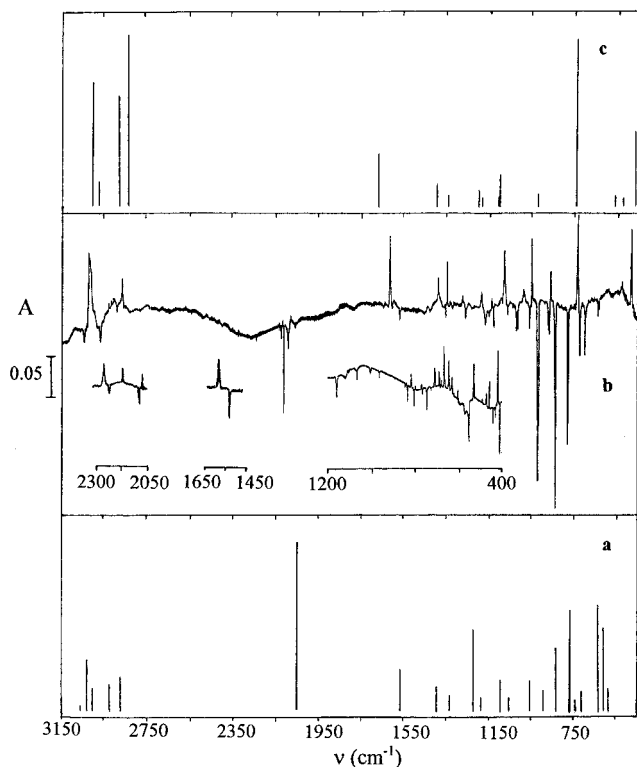


Figure 4. IR spectra (Ar, 12 K): (a) **6b**, calculated; (b) difference of the spectrum of the sample of Figure 1b (solid line) before (positive) and after (negative) further irradiation with 454 or 254 nm light (deuterated species in inset); (c) **2b**, calculated.

spectrum (at 250 and 480 nm). Additional support for the identification of **2b** proposed above is provided by the absence of Ge–H stretching bands in its IR spectrum and by the reasonable agreement of the frequencies calculated for **2b** (Figure 4c) with the observed spectral features of this species (Figure 4b, positive peaks), and we consider it established.

As noted above, the conversion of germylene **2b** into the 301 nm photoproduct is found to be photoreversible and analogous to interconversion of silylene **2a** with 2*H*-silole (1-silacyclopenta-1,3-diene) **6a**.⁵ This similarity, as well as the observation of a prominent IR peak of the 301 nm photoproduct at 2115 cm⁻¹ in the Ge(sp²)–H stretching region, and a deuterium isotopic shift of this peak to 1536 cm⁻¹ in agreement with the calculated spectra of **6b** and **6b-d₆** (Figure 4a and Tables 5 and 9) strongly suggest an assignment of the 301 nm product to 2*H*-germole **6b**.

In summary, we consider the assignments of the 272 nm (2096 cm⁻¹) species as **1b** and of the 370–460 nm species as **2b** to be firm and the assignments of the 262 nm (2127 cm⁻¹) species as **5b** and the 301 nm (2115 cm⁻¹) species as **6b** to be very likely but conceivably reversed.

Discussion

Mechanistic Aspects. Germylene-to-Germene Interconversion. The products of photodecomposition of diazides **4a,b** and their photochemical transformations are shown in Scheme 1, which we believe best describes the chemistry both studied earlier for **1a**, **2a**, **4a**, **5a** and **6a** and observed in the present work for **1b**, **2b**, **4b**, **5b**, and **6b**. The absorption of the precursor **4b**

Table 1. Calculated Relative Energies (kcal/mol) of C₄H₆Ge Isomers, Germene and Methylgermylene

C ₄ H ₆ Ge ^a		CH ₄ Ge ^b	
isomer	Δ <i>E</i>	isomer	Δ <i>E</i>
1b	0	CH ₃ GeH	0
2b	2	H ₂ Ge=CH ₂	15–25
5b	27		
6b	25		

^a Present work. ^b References 13a and 18.

Table 2. Vibrations of 1-Germacyclopenta-2,4-diene (1*H*-Germole; **1b**)

mode	sym	freq (cm ⁻¹)		assign
		calcd (int) ^a	obsd	
<i>v</i> ₁	a ₁	3029 (7.89)		=C–H sym stretch
<i>v</i> ₂		3001 (25.0)	3015	=C–H sym stretch
<i>v</i> ₃		1980 (155)	2099	GeH ₂ sym stretch
<i>v</i> ₄		1542 (4.58)	1532	C=C sym stretch
<i>v</i> ₅		1325 (8.27)	1321	in-plane C–H bend
<i>v</i> ₆		1074 (5.26)	1064	C–H scissor (in-phase)
<i>v</i> ₇		898 (8.17)		C–C stretch
<i>v</i> ₈		853 (127)	906	GeH ₂ scissor
<i>v</i> ₉		682 (0.28)		C–Ge–C sym stretch
<i>v</i> ₁₀		384 (19.1)		C–Ge–C bend
<i>v</i> ₁₁	a ₂	1014 (0)		=C–H twist (out-of-phase)
<i>v</i> ₁₂		764 (0)		=C–H wag (out-of-phase)
<i>v</i> ₁₃		633 (0)		GeH ₂ twisting
<i>v</i> ₁₄		366 (0)		GeH ₂ twist, C=C–C=C twist
<i>v</i> ₁₅	b ₁	1963 (149)	2096	GeH ₂ asym stretch
<i>v</i> ₁₆		1010 (0.36)	1031	=C–H twist (in-phase)
<i>v</i> ₁₇		708 (222)	722	=C–H wag (in-phase)
<i>v</i> ₁₈		493 (15.3)	505	GeH ₂ rock, CH wag (in-phase)
<i>v</i> ₁₉		246 (0.33)		out-of-plane GeH ₂ scissor, CH twist (in-phase)
<i>v</i> ₂₀	b ₂	3027 (12.1)		=C–H asym stretch
<i>v</i> ₂₁		2989 (6.90)		=C–H asym stretch
<i>v</i> ₂₂		1587 (7.63)	1593	C=C asym stretch
<i>v</i> ₂₃		1270 (5.02)	1285	in-plane =C–H bend
<i>v</i> ₂₄		1085 (0.88)	1168	=C–H scissor (out-of-phase)
<i>v</i> ₂₅		802 (81.8)	783	GeC–H rock (out-of-phase)
<i>v</i> ₂₆		660 (22.0)	682	GeH ₂ wag
<i>v</i> ₂₇		509 (11.1)		C–Ge–C asym stretch

^a Intensity, in km/mol.

peaks at 232 nm in the UV region, and it readily decomposes when irradiated with 248 or 254 nm light. There is no wavelength at which **4b** could be irradiated without exposing its primary photoproduct **2b** to further photoconversion, since **2b** absorbs at 248 nm. Since the products of the secondary photochemical processes all absorb more or less strongly at 248 and 254 nm, the initial photochemical destruction of **4b** produces a steady state in which **1b**, **2b**, **5b**, and **6b** are all present to some degree. Subsequent irradiation at various wavelengths changes the steady-state composition in ways that allowed us to separate the spectral characteristics of the four constituents. The assignment of the four structures is based on analogy to the previously studied silicon analogues, on consideration of the spectral characteristics, and on comparison with calculations. As noted, the evidence for the assignment of **1b** and **2b** is strong, while that for **5b** and **6b** is weaker in that they could possibly have been interchanged.

We believe that the germole **1b** is being formed from germylene **2b** via **6b** and **5b** by a 1,2-H shift followed by two consecutive photochemically allowed 1,3-H shifts, the same as in the case of silicon analogues. We cannot exclude the possibility that a photochemically forbidden 1,5-H shift takes **6b** directly to **1b**. There might also be a direct photochemical path from **2b** to **1b**, proceeding by an attack of divalent germanium on the C=C double bond in an envelope conformation of the elec-

Table 3. Vibrations of 1-Germacyclopent-3-ene-1,1-diyl (2b)

mode	sym	freq (cm ⁻¹)		assign
		calcd (int) ^a	obsd	
ν_1	a ₁	2991 (50.4)	3017	=C-H sym stretch
ν_2		2823 (2.23)		CH ₂ sym stretch
ν_3		1662 (21.9)	1615	C=C stretch
ν_4		1385 (0.07)		CH ₂ bend (in-phase)
ν_5		1206 (7.22)	1186	=C-H sym rock
ν_6		1095 (13.3)	1078	CH ₂ rock (in-phase)
ν_7		882 (0.1)		C-C sym stretch
ν_8		560 (4.78)	508	C-Ge-C sym stretch
ν_9		354 (23.8)		C-Ge-C bend
ν_{10}	a ₂	2862 (0)		CH ₂ asym stretch
ν_{11}		1100 (0)		CH ₂ twist (out-of-phase)
ν_{12}		971 (0)		=C-H twist
ν_{13}		599 (0)		CH ₂ rock, CH ₂ twist
ν_{14}		320 (0)		CH ₂ rock, C=C rock
ν_{15}	b ₁	2865 (45.6)	2908	CH ₂ asym stretch (in-phase)
ν_{16}		1098 (4.97)		CH ₂ twist (in-phase)
ν_{17}		744 (57.7)	732	=C-H wag
ν_{18}		531 (3.25)		CH ₂ twist
ν_{19}		65 (1.63)		C-Ge-C rock
ν_{20}	b ₂	2966 (9.83)		=C-H asym stretch
ν_{21}		2822 (69.8)	2865	CH ₂ sym stretch (out-of-phase)
ν_{22}		1381 (9.23)	1389	CH ₂ bend (out-of-phase)
ν_{23}		1335 (2.59)	1346	=C-H rock
ν_{24}		1183 (4.09)		CH ₂ rock (out-of-phase)
ν_{25}		917 (6.34)	949	C-C asym stretch
ν_{26}		732 (0.22)		C-C=C-C asym bend
ν_{27}		451 (29.3)	478	C-Ge-C asym stretch

^a Intensity, in km/mol.**Table 4. Vibrations of 1-Germacyclopenta-1,4-diene (3H-Germole; 5b)**

mode	sym	freq (cm ⁻¹)		assign
		calcd (int) ^a	obsd	
ν_1	a'	3049 (1.65)		(Ge=C)-H stretch
ν_2		3031 (11.9)		=C-H sym stretch
ν_3		2989 (14.0)		=C-H asym stretch
ν_4		2833 (35.9)		CH ₂ sym stretch
ν_5		2052 (90.0)	2127	Ge-H stretch
ν_6		1548 (14.9)	1553	C=C stretch
ν_7		1401 (4.15)		CH ₂ bend
ν_8		1313 (1.49)		in-phase C-H rock
ν_9		1274 (20.7)		in-phase CH ₂ -CH=CH rock
ν_{10}		1196 (10.0)		Ge=C asym stretch
ν_{11}		1063 (4.61)		=C-H rock
ν_{12}		967 (4.84)		CH ₂ -CH scissor
ν_{13}		843 (7.65)	834	Ge=C sym stretch
ν_{14}		822 (36.3)	787	in-plane (Ge)=CH rock, H-Ge-C-H rock
ν_{15}		753 (7.02)		CH ₂ -CH=CH bend, Ge-CH stretch
ν_{16}		619 (10.4)		in-plane Ge-H rock
ν_{17}		586 (24.2)		Ge-C stretch
ν_{18}		388 (22.2)		C=Ge-C stretch
ν_{19}	a''	2870 (20.8)		CH ₂ asym stretch
ν_{20}		1126 (2.88)		CH ₂ twist
ν_{21}		978 (0)		=C-H twist
ν_{22}		898 (15.1)		(in-phase) =C-H rock
ν_{23}		657 (83.6)	682	out-of-plane (Ge)=C-H wag
ν_{24}		649 (18.3)	635	CH ₂ rock
ν_{25}		412 (0.55)		out-of-plane Ge-H rock
ν_{26}		356 (0.22)		out-of-plane CH ₂ -CH=CH wag
ν_{27}		262 (13.8)		CH ₂ -CH torsion

^a Intensity, in km/mol.

tronically excited state of **2b**. This latter possibility is suggested by the observation of the formation of **1b** as a minor byproduct during the conversion of **2b** into **6b** by irradiation with visible (454 nm) light, absorbed only by **2b**. An alternative way of accounting for this result is to postulate the hot ground-state reaction **6b** → **1b**, i.e., a thermal 1,5-H shift in **6b** immediately after its photogeneration from **2b**, before it has vibrationally equilibrated with the surrounding matrix. The ground-state-allowed 1,5-H shift should be quite facile, given

Table 5. Vibrations of 1-Germacyclopenta-1,3-diene (2H-Germole; 6b)

mode	sym	freq (cm ⁻¹)		assign
		calcd (int) ^a	obsd	
ν_1	a'	3053 (2.37)		GeC-H stretch
ν_2		3021 (22.2)	3048	=C-H sym stretch
ν_3		3000 (8.96)		=C-H asym stretch
ν_4		2862 (12.8)	2894	CH ₂ sym stretch
ν_5		2055 (68.0)	2115	Ge-H stretch
ν_6		1562 (15.3)	1574	C=C stretch
ν_7		1379 (10.0)		CH ₂ bend
ν_8		1335 (6.57)	1352	=C-H rock
ν_9		1216 (32.3)	1262	Ge=C-C asym stretch, GeC-H in-plane rock
ν_{10}		1167 (6.10)		CH ₂ wag, Ge-CH ₂ -CH asym stretch
ν_{11}		1087 (11.7)		CH ₂ -CH, CH-CH in-phase scissor
ν_{12}		953 (12.8)	959	CH-CH stretch, C-H rock
ν_{13}		890 (8.31)	922	CH ₂ -CH stretch, CH ₂ rock
ν_{14}		830 (22.3)	838	Ge=C-C sym stretch
ν_{15}		750 (4.82)		CH ₂ -CH=CH bend, Ge-CH ₂ stretch
ν_{16}		599 (33.4)	631	in-plane Ge-H rock
ν_{17}		572 (9.84)		Ge-C stretch
ν_{18}		382 (3.37)		C-Ge=C bend
ν_{19}	a''	2912 (10.4)	2972	CH ₂ asym stretch
ν_{20}		1057 (5.55)		CH ₂ twist
ν_{21}		978 (0.05)		=C-H twist
ν_{22}		769 (41.4)	778	out-of-plane GeC-H rock
ν_{23}		712 (8.10)		out-of-plane C-C=C wag
ν_{24}		620 (41.9)	698	out-of-plane CH ₂ wag, =CH wag
ν_{25}		452 (15.1)		HC-CH torsion
ν_{26}		364 (2.18)		CH ₂ rock, out-of-plane Ge-H rock
ν_{27}		132 (0.79)		ring deformation

^a Intensity, in km/mol.**Table 6. Vibrations of 1-Germacyclopenta-2,4-diene-d₆ (1H-Germole-d₆; 1b-d₆)**

mode	sym	freq (cm ⁻¹)		assign
		calcd (int) ^a	obsd	
ν_1	a ₁	2252 (9.24)	2262	in-phase =C-D sym stretch
ν_2		2214 (9.48)	2229	in-phase =C-D asym stretch
ν_3		1519 (5.22)		C=C sym stretch
ν_4		1406 (82.4)	1522	GeD ₂ sym stretch
ν_5		1148 (5.42)	1168	C-C stretch, D-(CGeC)-D in-plane rock
ν_6		777 (0.92)		C-C stretch, D-(C-C)-D scissor
ν_7		766 (5.71)		in-phase =C-D scissor
ν_8		614 (3.34)		C-Ge-C sym stretch
ν_9		608 (67.1)	641	GeD ₂ scissor
ν_{10}		374 (16.1)		C-Ge-C bend
ν_{11}	a ₂	834 (0)		out-of-phase =C-D scissor
ν_{12}		606 (0)		out-of-phase =C-D wag
ν_{13}		483 (0)		GeD ₂ twist
ν_{14}		290 (0)		ring twist
ν_{15}	b ₁	1400 (79.9)	1507	GeD ₂ asym stretch
ν_{16}		794 (3.46)		in-phase =C-D twist
ν_{17}		542 (140)	594	in-phase =C-D wag
ν_{18}		384 (3.57)		C-Ge-C wag
ν_{19}		203 (0.01)		ring deformation
ν_{20}	b ₂	2249 (3.48)		out-of-phase =C-D sym stretch
ν_{21}		2206 (3.64)		out-of-phase =C-D asym stretch
ν_{22}		1532 (9.94)		C=C asym stretch
ν_{23}		1024 (0.08)		in-phase =C-D rock
ν_{24}		839 (15.4)	878	D-(C-C)-D rock
ν_{25}		683 (29.9)	707	D-(CGeC)-D in-plane scissor
ν_{26}		494 (0.26)		C-Ge-C asym stretch
ν_{27}		473 (30.1)	486	GeD ₂ wag

^a Intensity, in km/mol.

its large exothermicity. According to our RHF (DZ+d) calculations, 1H-germole **1b** is the most thermodynamically stable of the four isomers (Table 1), with the germylene isomer **2b** being less stable only by 2 kcal/mol, while the germadiene isomers, **6b** and **5b**, are much less stable (by 25 and 27 kcal/mol, respectively).

The formation of another germadiene isomer, **5b** (UV band at 262 nm), clearly seen after irradiation of

Table 7. Vibrations of 1-Germacyclopent-3-ene-1,1-diyl- d_6 (2b- d_6)

mode	sym	freq (cm ⁻¹)		assign
		calcd (int) ^a	obsd	
ν_1	a ₁	2229 (16.5)	2256	=C-D sym stretch
ν_2		2056 (0.87)		in-phase CD ₂ sym stretch
ν_3		1619 (26.2)	1579	C=C stretch
ν_4		1059 (7.42)	1072	CD ₂ -CD sym stretch
ν_5		1001 (5.31)		in-phase CD ₂ bend
ν_6		811 (0.91)	804	in phase =C-D rock
ν_7		736 (5.89)	748	in-phase CD ₂ wag
ν_8		505 (1.88)		C-Ge-C sym stretch
ν_9		343 (22.4)		C-Ge-C bend
ν_{10}	a ₂	2115 (0)		out-of-phase CD ₂ asym stretch
ν_{11}		891 (0)		CD ₂ -C=C-CD ₂ twist
ν_{12}		718 (0)		D-(C=C)-D twist
ν_{13}		477 (0)		ring deformation
ν_{14}		258 (0)		C=C twist
ν_{15}	b ₁	2119 (29.6)	2171	in-phase CD ₂ asym stretch
ν_{16}		847 (8.87)	837	CD ₂ twist
ν_{17}		554 (28.6)	551	D-(C=C)-D wag
ν_{18}		409 (2.56)		in-phase CD ₂ -CD rock
ν_{19}		56 (1.14)		out-of-plane C-Ge-C wag
ν_{20}	b ₂	2186 (3.81)		=C-D asym stretch
ν_{21}		2055 (27.7)	2077	out-of-phase CD ₂ sym stretch
ν_{22}		1172 (0.01)	1164	CD ₂ -CD asym stretch
ν_{23}		1010 (9.71)	1024	out-of-phase CD ₂ bend
ν_{24}		991 (4.26)	976	out-of-phase CD ₂ rock, in-plane =C-D rock
ν_{25}		748 (1.62)	772	in-plane asym =C-D rock
ν_{26}		656 (5.54)		out-of-phase CD ₂ -CD scissor
ν_{27}		416 (23.0)	438	C-Ge-C asym stretch

^a Intensity, in km/mol.**Table 8. Vibrations of 1-Germacyclopenta-1,4-diene- d_6 (3H-Germole- d_6 , 5b- d_6)**

mode	sym	freq (cm ⁻¹)		assign
		calcd (int) ^a	obsd	
ν_1	a'	2253 (6.98)		in-phase =C-D sym stretch
ν_2		2250 (2.49)		out-of-phase =C-D sym stretch
ν_3		2206 (3.99)		=C-D asym stretch
ν_4		2065 (14.9)	2068	CD ₂ sym stretch
ν_5		1508 (20.8)		C=C stretch
ν_6		1462 (46.8)	1547	Ge-D stretch
ν_7		1184 (10.5)		CD-CD ₂ -CD asym stretch
ν_8		1119 (2.09)		Ge=C asym stretch, CD ₂ bend
ν_9		1028 (2.81)		CD ₂ -CD, =C-D out-of-phase rock
ν_{10}		1020 (5.94)	1072	CD ₂ bend
ν_{11}		795 (9.25)		=C-D scissor
ν_{12}		763 (12.4)		in-phase C=Ge sym stretch, CD ₂ -CD stretch
ν_{13}		737 (6.48)		in-phase CD ₂ -CD, =C-D scissor
ν_{14}		679 (8.47)	686	out-of-phase Ge=C, CD ₂ CD stretch
ν_{15}		659 (2.34)		D-(CGeC)-D rock
ν_{16}		561 (10.0)		Ge-C stretch
ν_{17}		445 (20.3)		in-plane Ge-D rock
ν_{18}		377 (18.2)		C=Ge-C bend
ν_{19}	a''	2126 (12.5)		CD ₂ asym stretch
ν_{20}		867 (2.05)		CD ₂ -CD(=CD) torsion
ν_{21}		781 (1.92)		CD ₂ wag
ν_{22}		727 (8.14)		CD ₂ rock, =C-D twist
ν_{23}		494 (0.04)		out-of-phase =C-D wag
ν_{24}		483 (62.4)	509	in-phase CD ₂ -CD, =C-D wag
ν_{25}		326 (1.22)		out-of-plane CD=CD-Ge wag
ν_{26}		277 (0.19)		out-of-plane Ge-D rock
ν_{27}		227 (8.53)		CD ₂ -CD(=Ge) torsion

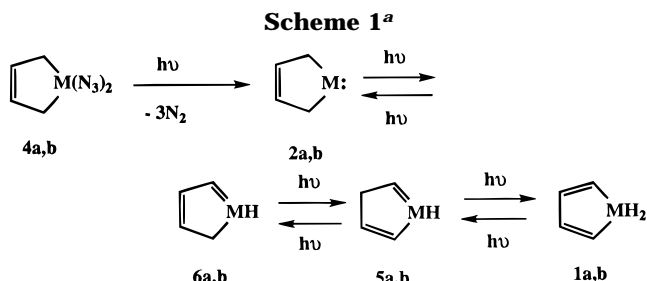
^a Intensity, in km/mol.

germole **1b** (UV absorption at 272 nm) with 308 nm light, is reasonably explained by a photochemically allowed 1,3-H shift by analogy with the known⁵ photoconversion of the silole **1a** into **5a**.

The photochemical conversion of group 14 carbene analogues to their double-bonded structural isomers by a 1,2-H shift has been experimentally established only for alkylsilylenes^{5,8} and not for their heavier group 14

Table 9. Vibrations of 1-Germacyclopenta-1,3-diene- d_6 (2H-Germole- d_6 ; 6b- d_6)

mode	sym	freq (cm ⁻¹)		assign
		calcd (int) ^a	obsd	
ν_1	a'	2257 (2.15)		(Ge=C)-D stretch
ν_2		2245 (7.38)		=C-D sym stretch
ν_3		2212 (5.74)	2232	=C-D asym stretch
ν_4		2038 (4.62)	2090	CD ₂ sym stretch
ν_5		1517 (15.1)		C=C stretch
ν_6		1462 (43.2)	1536	Ge-D stretch
ν_7		1192 (20.3)		CD ₂ -(C=C)-CD asym stretch
ν_8		1069 (14.6)		Ge=C-C asym stretch
ν_9		1016 (3.44)		CD ₂ scissor, =C-D in-phase rock
ν_{10}		988 (6.21)		CD ₂ wag + Ge-C-C asym stretch
ν_{11}		833 (5.64)		in-plane (CD ₂)C-D rock
ν_{12}		780 (8.15)	820	in-plane (CD ₂)C-D rock
ν_{13}		735 (3.79)		CD ₂ -CD scissor
ν_{14}		696 (8.68)	691	Ge=C-C sym stretch
ν_{15}		665 (10.1)	663	CD ₂ -CD=CD in-plane bend
ν_{16}		532 (8.23)	529	Ge-CD ₂ stretch
ν_{17}		437 (21.1)	454	in-plane Ge-D rock
ν_{18}		368 (1.64)		C-Ge=C bend
ν_{19}	a''	2157 (6.01)		CD ₂ asym stretch
ν_{20}		837 (5.05)		CD ₂ twist, D-(C=C)-D twist
ν_{21}		767 (1.25)		CD ₂ twist, (Ge=C-)C-D in-plane rock
ν_{22}		599 (17.6)	621	C-Ge=C twist
ν_{23}		561 (0.29)		CD ₂ twist, ring deformation
ν_{24}		479 (31.0)	465	out-of-plane D-(C=C-C)-D wag
ν_{25}		371 (13.8)	416	(CD)=CD out-of-plane wag
ν_{26}		270 (0.82)		out-of-plane Ge-D rock
ν_{27}		108 (0.64)		ring deformation

^a Intensity, in km/mol.^a Legend: **a**, M = Si; **b**, M = Ge.

analogues. A recent attempt to produce 1-methylgermene, CH₃(H)Ge=CH₂, by irradiation of a matrix sample of dimethylgermylene with visible light was unsuccessful.⁹ This might be related to the fact that calculations predict a higher ground-state thermodynamic stability for alkylgermylenes than for the isomeric germenes. For instance, CH₃GeH is computed to be 15–25 kcal/mol more stable than the H₂Ge=CH₂ isomer (Table 1). In contrast, the isomerizations of alkylsilylenes and silenes are nearly thermoneutral (e.g. CH₃SiH vs H₂Si=CH₂¹⁹). The less favorable energetics may cause the excited potential energy surface to acquire an unfavorable slope in the case of germynes, preventing the excited molecule from reaching the return point to the ground state that leads to isomerization. To our knowledge, the presently observed germylene-to-germene photoisomerization is the first experimentally proved example. The conjugation provided by the additional double bond could well be responsible for the difference.

A. 1H-Germole 1b. Molecular Geometry. Our calculations predict a planar *C*_{2v} geometry, similar to

(19) Gordon, M. S. In *Molecular Structure and Energetics*; Liebman, J. F., Greenberg, A., Eds.; VCH: Deerfield Beach, FL, 1986; Vol. 1, Chapter 4, pp 101–122, and references therein.

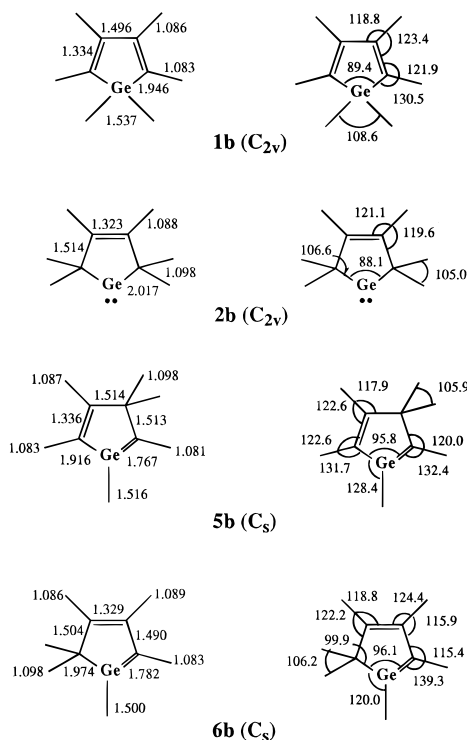


Figure 5. Calculated equilibrium geometries of **1b**, **2b**, **5b**, and **6b**, giving symmetry, bond lengths (Å), and valence angles (deg).

the geometries of the silicon analogue **1a** and of 1,3-cyclopentadiene (**7**). The C=C (1.334 Å) and C–C (1.496 Å) bond lengths in **1b** are calculated to be the same as those in 1*H*-silole **1a** (1.33 and 1.49 Å, respectively)^{5c} and very close to those in **7** (1.32 and 1.44 Å, respectively)²⁰ and to X-ray-determined ones in C-phenylated germoles (1.35 and 1.51 Å, respectively). The optimized C–Ge–C bond angle (89.4°) is also close to the C–Si–C angle calculated earlier^{5c} for 1*H*-silole (~92°) and to experimentally determined ones in heavily substituted germoles (90–91°)² and is smaller than the C–C–C bond angle (102°) in **7**. The Ge–C bond length in **1b** is calculated to be 1.946 Å, which is within the range of experimentally established values for a single Ge–C bond in substituted germoles (1.92–1.98 Å)² and in methylgermane (1.945 Å).²¹ The H–Ge–H bond angle in **1b** is calculated to be close (108.6°) to a standard value (~109°) for the sp³-hybridized configuration of the central atom (Figure 5).

UV Spectrum. The assignment of the band at 272 nm in the UV spectrum of **1b** to a π – π^* transition seems quite obvious, since this transition is normally found² at 280–286 nm in the UV spectra of C-alkylated siloles, germoles, and phospholes, while 1*H*-silole **1a** exhibits a π – π^* transition at 278 nm.^{5c}

IR Spectrum. A full assignment of the experimental bands in the IR spectrum of **1b** has been suggested by comparison with the IR spectra of **7**,²² germacyclopentane (**8**) and its 1,1-dideuterio derivative,^{23a} 1,1,3,4-

tetramethylgermole¹⁶ (**9**), and 1*H*-silole (**1a**),^{5c} and the *ab initio* calculated vibrational spectra of **1b** and **1b-d₆** and by the analysis of the isotopic band shifts in the spectrum of **1b-d₆**. The molecule of **1b** has 27 normal vibrational modes; four of them have *a₂* symmetry and are forbidden in the IR spectrum. Two of the ring skeleton vibrations in **1b**, and three of those in **1b-d₆**, calculated to lie below 400 cm⁻¹, could not be observed in our experiments. In the 400–4000 cm⁻¹ spectral region we have found 16 out of the 21 expected fundamentals in **1b** and 10 out of 20 in **1b-d₆**.

A band at 3015 cm⁻¹, found for **1b** in the IR region above 3000 cm⁻¹, undoubtedly belongs to a =C–H stretching vibration. This agrees with the calculated spectrum of **1b** (Table 2) and with our previous data^{5c} for silole **1a** and literature data for **7**²² and **9**.¹⁶ Our calculations predict the shift of the =C–D stretching bands in the IR spectrum of **1b-d₆** to the 2200–2260 cm⁻¹ region. Therefore, we believe that the two bands at 2229 and 2262 cm⁻¹ found in this spectrum are due to =C–D stretching vibrations. A strong band at 2096 cm⁻¹ with a shoulder at 2099 cm⁻¹ in the spectrum of **1b** and prominent peaks at 1507 and 1522 cm⁻¹ in the spectrum of **1b-d₆** are assigned to the antisymmetric and symmetric Ge–H and Ge–D stretches, respectively. They are observed in the spectra of **8** and **8-d₂** at 2066 cm⁻¹ and as a 1485, 1489 cm⁻¹ pair, respectively,^{23a} and are expected to be ~20–30 cm⁻¹ higher in **1b** and **1b-d₆** by analogy to an increase in the Si–H stretching frequency in **1a**^{5c} relative to silacyclopentane.^{23b}

The bands of symmetric and antisymmetric C=C stretches have been found in the 1480–1580 cm⁻¹ region of the IR spectrum of matrix-isolated **7**²² and at 1478 and 1608 cm⁻¹ in the spectrum of silole **1a**,^{5c} while in the spectrum of **9** only one band at 1520 cm⁻¹ has been observed.¹⁶ According to these data and to our calculations (Table 2) it seems reasonable to assign the bands at 1532 and 1593 cm⁻¹ to a symmetric and antisymmetric C=C stretch, respectively.

The in-plane =C–H bending frequencies are located in the 1240–1385 cm⁻¹ region for **7**²² and for **1a**,^{5c} where the latter shows two bands at 1285 and 1346 cm⁻¹. In the IR spectrum of **1b** two bands at 1285 and 1321 cm⁻¹ are assigned to this vibrational mode, in good agreement with the calculated values at 1270 and 1325 cm⁻¹ (Table 2). The latter band is shifted to 1168 cm⁻¹ in the spectrum of **1b-d₆**, in agreement with the calculations and with literature data for **7** and **7-d₆**.²²

Three bands in the 1000–1200 cm⁻¹ region in the spectrum of **1b** at 1031, 1064, and 1168 cm⁻¹ are assigned to the in-plane =C–H bending modes coupled with ring vibrations. This assignment agrees with the calculations (Table 2) and with the spectral data for **1a**.^{5c} In the spectrum of **1b-d₆** those bands are expected to shift to the 700–1000 cm⁻¹ region according to literature data on **7-d₆**²² and our calculations (Table 6). Therefore, two bands at 707 and 878 cm⁻¹ found in the spectra of **1b-d₆** were assigned to the in-plane =C–D bending modes coupled with ring C–C vibrations. One more band, at 783 cm⁻¹ in **1b**, is assigned to the C–H rocking mode strongly coupled with ring vibration and GeH₂ bending motions.

The calculations (Table 2) predict a value of 853 cm⁻¹ for the GeH₂ scissoring mode frequency and a shift to 608 cm⁻¹ in **1b-d₆**. This is in reasonable agreement

(20) O'Sullivan, P. S.; Hameka, H. F. *Chem. Phys. Lett.* **1969**, *4*, 123.

(21) Harmony, M. D.; Laurie, V. W.; Kuczowski, R. L.; Schwendeman, R. H.; Ramsay, D. A.; Lovas, F. J.; Lafferty, W. J.; Maki, A. G. *J. Phys. Chem. Ref. Data* **1979**, *8*, 619.

(22) Ball, D. W.; Kafafi, Z. H.; Hauge, R. H.; Margrave, J. L. *Inorg. Chem.* **1985**, *24*, 3708.

(23) (a) Durig, J. R.; Willis, J. N., Jr. *J. Chem. Phys.* **1970**, *52*, 6108.

(b) Durig, J. R.; Willis, J. N., Jr. *J. Mol. Struct.* **1969**, *32*, 320.

with the shift from 881 to 631 cm^{-1} in going from **8** to **8-d₂**^{23a} and with the observation of intense bands at 906 cm^{-1} for **1b** and 641 cm^{-1} for **1b-d₆**. The frequency of the GeH₂ wagging mode is known to shift from 694 cm^{-1} in **8** to 514 cm^{-1} in **8-d₂** and is also calculated to shift from 660 cm^{-1} in **1b** to 473 cm^{-1} in **1b-d₆**. These data are in good agreement with the assignment of bands at 682 cm^{-1} in **1b** and at 486 cm^{-1} in **1b-d₆** to the GeH₂ and GeD₂ wagging modes, respectively. The GeH₂ and GeD₂ twisting modes in **1b** and **1b-d₆** are forbidden in the IR and were not expected to be observed in our spectra. As shown by calculations (Table 2), the GeH₂ rocking mode in **1b** should be strongly mixed with the =C–H wagging motion, and this accounts for its higher frequency (505 cm^{-1}) in **1b** than in **8** (431 cm^{-1}).

The assignment of the most intense band at 722 cm^{-1} in the spectrum of **1b** to the =C–H wagging mode is in good agreement with the calculated value of 708 cm^{-1} (Table 2) and with the value of 713 cm^{-1} in **1a**.^{5c} It also agrees with the observed isotopic shift to 594 cm^{-1} in **1b-d₆**, for which the calculated value is 542 cm^{-1} (Table 6). The weak band at 527 cm^{-1} is assigned to an antisymmetric Ge–C stretch, since this frequency is close to the calculated value of 509 cm^{-1} for **1b** and to an antisymmetric Ge–C stretch in **8**^{23a} at 481 cm^{-1} , which shows some coupling with the GeH₂ bending motions.

B. Germylene 2b. Molecular Geometry. The calculations for the singlet ground state of **2b** yield an optimized C_{2v} planar structure with a Ge–C bond length of 2.017 Å, close to that calculated²⁴ for dimethylgermylene (2.024 Å), a C=C bond length of 1.323 Å, the same as in the silicon analogue **2a**,^{5c} and a C–Ge–C bond angle of 88.1° (Figure 5), close to that calculated^{5c} for silylene **2a** (90.4°) and smaller than calculated²⁴ for dimethylgermylene (97.8°).

UV–Vis Spectrum. The germylene **2b** exhibits two bands at 248 and 370–460 nm, similar to those of the silylene **2a** at 250 and 480 nm.⁵ The broad visible absorption band at 480 nm for **2a** was assigned to an n(Si) → p(Si) transition on the basis of CI calculations.^{5c} We believe that the similarity of the structures of **2b** and **2a** and the closeness of the maxima of visible absorption of **2b** and dimethylgermylene⁹ (in an Ar matrix, a peak at 405 nm,⁹ in reasonable agreement with *ab initio* calculations²⁴) leave no doubt that the 370–460 nm band in the spectrum of **2b** can be safely assigned to an n(Ge) → p(Ge) transition.

On the basis of CI calculations,^{5c} the band at 250 nm in **2a**, not observed for saturated silylenes, has been attributed to a transition to a state in which an n(Si) → π* configuration makes a significant contribution. We propose a similar assignment of the 248 nm band that is observed in the UV spectrum of **2b** and is absent in dimethylgermylene.⁹

IR Spectrum. In **2b** five out of 27 vibrations are IR-forbidden. Two other frequencies calculated to lie below 400 cm^{-1} in both **2b** and **2b-d₆** would not be detectable in our experiments. We found 12 bands in the IR spectrum of **2b** (Table 3) and 14 bands in that of **2b-d₆** (Table 7). The assignment of these bands is based on the calculated vibrational spectra of **2b** and **2b-d₆** and

on comparison with the IR spectra of **2a**, cyclopentene,²⁵ **8**,^{23a} and dimethylgermylene.⁹

Only one band of **2b** was found to lie above 3000 cm^{-1} in the =C–H stretching region. This is a strong band at 3017 cm^{-1} , shifted to 2256 cm^{-1} in the spectrum of **2b-d₆**. These values are in good agreement with the calculated frequencies of 2991 and 2229 cm^{-1} (Tables 3 and 7) and are assigned to the =C–H and the =C–D symmetric stretching vibrations, respectively.

Two bands, observed at 2908 and 2865 cm^{-1} in the spectrum of **2b** and at 2171 and 2077 cm^{-1} in that of **2b-d₆**, should be assigned to ring CH₂ and CD₂ stretches, respectively, according to the calculations (Tables 3 and 7) and to literature data for **8**^{23a} and **2a**,^{5c} which indicate that the CH₂ stretches appear in the 2910–2980 and 2860–2880 cm^{-1} regions.

A strong band at 1615 cm^{-1} is assigned to the C=C stretch in **2b**. This assignment agrees well with the location of the C=C stretches in the spectra of cyclopentene²⁵ (1611–1617 cm^{-1}) and **2a**^{5c} (1624 cm^{-1}). The calculations predict the shift of this band to lower frequencies in the spectrum of the deuterium-labeled molecule **2b-d₆**, and we assign the band at 1579 cm^{-1} (Table 7) to the C=C stretch in **2b-d₆**.

A medium-intensity band at 1389 cm^{-1} in **2b** (1024 cm^{-1} in **2b-d₆**) is assigned to the b₂ CH₂ (CD₂) bending mode, since the calculations predict a value of 1381 cm^{-1} for **2b** and 1010 cm^{-1} for **2b-d₆**, and in **8**^{23a} this mode is observed at 1415 cm^{-1} . In **2a** the b₂ in-plane =C–H asymmetric rocking mode is located at 1397 cm^{-1} . The calculations predict a value of 1335 cm^{-1} for **2b** and a shift to 991 cm^{-1} in **2b-d₆**, where this vibration is coupled with the out-of-phase CD₂ rocking mode of the same symmetry. The closest spectral features matching this are the bands at 1346 and 976 cm^{-1} observed in the spectra of **2b** and **2b-d₆**, respectively.

The CH=CH symmetric rocking mode of a₁ symmetry in **2a** is found at 1208 cm^{-1} . The calculations predict a value of 1206 cm^{-1} and a strong coupling with the CH₂ in-phase rocking mode for this mode in **2b** and a value of 811 cm^{-1} and a coupling both with the CD₂ in-phase rocking and with the C–C symmetric stretch modes for **2b-d₆**. This consideration gives the best match for the observed bands at 1186 and 804 cm^{-1} in the spectra of **2b** and **2b-d₆**, respectively.

Calculations for **2b** yield the 1095 cm^{-1} value for the in-phase CH₂ rocking mode of a₁ symmetry. The assignment of the band observed at 1078 cm^{-1} to this mode is also supported by the values of 1078 and 1108 cm^{-1} , respectively, observed for this mode in the spectra of **8**^{23a} and **2a**.^{5c}

The CH₂ twisting mode of b₁ symmetry is predicted at 1098 cm^{-1} for **2b** and at 847 cm^{-1} for **2b-d₆**. We did not observe any matching band in the spectrum of **2b**, but a medium-intensity band at 837 cm^{-1} in the spectrum of **2b-d₆** can be safely assigned to this mode.

Ring deformations involving C–C stretches are normally observed in cyclopentane at 1100–800 cm^{-1} . A prominent peak of **2b** at 949 cm^{-1} falls into this spectral region and agrees well with the calculated b₂ C–C mode at 917 cm^{-1} and with the value of 944 cm^{-1} observed earlier^{5c} for **2a**. According to calculations (Table 7), two

(24) Barthelat, J.-C.; Saint Roch, B.; Trinquier, G.; Satgé, J. *J. Am. Chem. Soc.* **1980**, *102*, 4080.

(25) Lin-Vien, D.; Colthup, N. B.; Fateley, W. G.; Grasselli, J. G. *The Handbook of Infrared and Raman Characteristic Frequencies of Organic Molecules*; Academic Press: San Diego, CA, 1991.

bands at 1072 and 1164 cm^{-1} , observed in **2b-d₆**, belong to the a_1 symmetric and the b_2 antisymmetric C–C stretches, respectively. A higher than usual frequency for the latter mode indicates its strong coupling with the CD_2 bending modes of similar frequency.

Two other bands at 748 and 772 cm^{-1} in **2b-d₆** could be assigned to the a_1 in-plane =C–D symmetric rocking mode coupled with in-phase CD_2 wagging and to the b_2 in-plane antisymmetric rocking mode, respectively. These agree well with the calculated =C–D values of 736 and 748 cm^{-1} for these modes (Table 7).

The most intense band at 732 cm^{-1} in **2b** should be attributed to the b_1 =C–H wagging mode, since it is found in the spectrum of **2a^{5c}** at 770 cm^{-1} and matches well both the calculated value at 744 cm^{-1} and the high intensity of this band (Table 3). In **2b-d₆**, this frequency is shifted to 551 cm^{-1} , in excellent accord with the calculated value at 554 cm^{-1} (Table 7).

The symmetric and antisymmetric C–Ge–C stretches in dimethylgermylene⁹ are observed at 541 and 527 cm^{-1} , respectively. For **2b** the calculations predict these frequencies to lie at 560 (a_1) and 451 cm^{-1} (b_2). This is in reasonable agreement with the observed bands of **2b** at 508 and 478 cm^{-1} . According to calculations those modes should be found in **2b-d₆** at 505 and 416 cm^{-1} . Since the b_2 C–Ge–C mode is predicted to show a much higher IR intensity, a band observed at 438 cm^{-1} in **2b-d₆** is attributed to this mode.

C. Germadienes (2H- and 3H-Germoles) 5b and 6b. Molecular Geometry. For both **5b** and **6b** our RHF calculations yielded a planar optimized geometry of C_s symmetry (Figure 5). The Ge=C bond lengths, 1.767 Å in **5b** and 1.782 Å in **6b**, are close to those calculated for $\text{H}_2\text{Ge}=\text{CH}_2$ (1.761 Å)²⁶ and for $(\text{CH}_3)_2\text{Ge}=\text{CH}_2$ (1.7613 Å).²⁷ The central Ge–C bond in the C=Ge–C=C fragment in **5b**, calculated to be 1.916 Å long, is shorter than the Ge–C bond in **6b** (1.974 Å) and in $(\text{CH}_3)_2\text{Ge}=\text{CH}_2$ (1.9803 Å).²⁷ This shortening clearly reflects the existence of conjugation of the two π -bonds in **5b**, similar to the C=Si–C=C π conjugation established earlier^{5c} for 1-silacyclopenta-1,4-diene (**5a**). Some degree of conjugation of the two π bonds in the Ge–C–C=C fragment of **6b** is also indicated by the slightly shorter central C–C bond length (1.490 Å) relative to other C–C bonds in **6b** (1.504 Å) and **5b** (1.513 and 1.514 Å). Significantly, the degree of shortening of the Ge–C and C–C central bonds in **5b** and **6b** is considerably smaller than that of the Si–C and C–C central bonds in their silicon analogues **5a** and **6a**, and this indicates that π conjugation is less effective in the germadienes than in the siladienes.

UV Spectra. We propose to assign the UV bands observed at 262 nm for **5b** and at 301 nm for **6b** to $\pi \rightarrow \pi^*$ transitions on the basis of comparison with their silicon analogues **5a** and **6a**. The red shifts of the UV bands of those siladienes relative to parent silene²⁸

suggested significant π -conjugation that we believe to be also present in germadienes **5b** and **6b** as discussed above on basis of optimized geometry, and as shown below by analysis of the IR spectra.

The large difference in the $\pi \rightarrow \pi^*$ excitation energies of **5b** (262 nm) and **6b** (301 nm) can be understood already at the simplest Hückel level by consideration of the molecular orbitals of *s-cis*-1,3-butadiene as a model while the Ge atom is placed in either the terminal or internal position. When the Ge atom is located in the terminal position, the reduction in the value of the GeC resonance integral relative to the CC resonance integral will affect only the C_3 – C_4 bond. Since at this bond the HOMO is bonding and the LUMO antibonding, the smaller value of the resonance integral reduces the HOMO–LUMO gap. When the Ge atom is in the internal position, the C_2 – C_3 bond is also affected. At this bond, the HOMO is antibonding and the LUMO bonding; therefore, the reduction of the resonance integral across this bond partially neutralizes the effect taking place across the C_3 – C_4 bond, and as a result, the HOMO–LUMO gap is less affected than when the Ge atom is in the terminal position.

A slightly lower $\pi \rightarrow \pi^*$ transition energy in **6b** relative to the silicon analogue **6a** (296 nm)⁵ correlates with the calculated^{18b} energies of these transitions in $\text{H}_2\text{Ge}=\text{CH}_2$ and $\text{H}_2\text{Si}=\text{CH}_2$, respectively, which indicate that the HOMO–LUMO gap is also slightly reduced in the former with respect to the latter.

IR Spectra. The calculated and observed frequencies of **5b** and **6b** are given in Tables 4 and 5, while those for their d_6 analogues are listed in Tables 8 and 9. Only one band out of the six IR-active =C–H stretches in **5b** and **6b** was observed in the spectrum of **6b** at 3048 cm^{-1} . The assignment of this band to the =C–H stretch agrees well with the calculated band intensity and frequency (3021 cm^{-1}). Five other =C–H stretches could not be detected, probably due to their low IR intensities. The =C–D stretches in **5b-d₆** and **6b-d₆** are calculated to lie within 2200–2260 cm^{-1} . The only band observed in this region and assigned to this mode was that of **6b-d₆** at 2232 cm^{-1} (Table 9). The symmetric and antisymmetric CH_2 stretches were observed only for **6b** at 2894 and 2972 cm^{-1} , while in **6b-d₆** and in **5b-d₆** the bands at 2090 and at 2068 cm^{-1} , respectively, were attributed to the symmetric CD_2 stretch.

Our calculations predict that the sp^2 Ge–H stretching modes should appear at frequencies higher than those of sp^3 Ge–H stretches in **1b** (Tables 2, 4, and 5) and thus they are expected to be observed above 2100 cm^{-1} in **5b** and **6b** and to shift by about 590 cm^{-1} to lower frequencies in **5b-d₆** and **6b-d₆**. A similar isotopic shift was observed for the pair **8** and **8-1,1-d₂**.^{23a} Therefore, we assigned the bands at 2127 and 2115 cm^{-1} to the =Ge–H stretches in **5b** and **6b** and those at 1547 and 1536 cm^{-1} to the =Ge–D stretches in **5b-d₆** and **6b-d₆**, respectively.

The calculations predict the appearance of the C=C stretching mode below 1600 cm^{-1} in **5b** and **6b** as well as in their d_6 analogues, similar to a location of this mode in the siladienes **5a** and **6a**. This is presumably a result of π conjugation and agrees with the assignment of the observed bands at 1553 cm^{-1} in the spectrum of **5b**, and at 1574 cm^{-1} in **6b**, to this vibrational mode.

(26) Windus, T. L.; Gordon, M. S. *J. Am. Chem. Soc.* **1992**, *114*, 9559.

(27) (a) Kudin, K.; Margrave, J. L.; Khabashesku, V. N. Ninth Summer Research Colloquium: Rice Quantum Institute, Aug 18, 1995; Rice Univ.: Houston, TX, 1995; Abstracts, p 26. (b) Khabashesku, V. N. Fargo Conference on Main Group Chemistry, May 30–June 1, 1996, Fargo, ND; North Dakota State Univ.: Fargo, ND, 1996; Abstracts, O-22. (c) Khabashesku, V. N. 2nd International Conference on Low Temperature Chemistry, Aug 4–9, 1996; Kansas City, MO; Durig, J., Klabunde, K., Eds.; Univ. of Missouri–Kansas City, BkMk Press: Kansas City, MO, 1996; Proceedings, pp 137–140. (d) Khabashesku, V. N.; Boganov, S. E.; Kudin, K. N.; Margrave, J. L.; Nefedov, O. M. To be submitted for publication.

Two weak bands at 1352 and 1262 cm^{-1} observed in the spectrum of **6b** were assigned to the in-plane =C–H rocking modes, in accord with the calculations (Table 5). In the spectrum of **6b-d₆**, the band observed at 820 cm^{-1} was attributed to the in-plane =C–D rocking mode. According to calculations, this mode is strongly coupled with other modes of the same symmetry in **6b-d₆**. No CH₂ bending vibrations were observed in the spectra of **5b** and **6b**, whereas in that of **5b-d₆** a band at 1072 cm^{-1} is assigned to the CD₂ bend, in accord with the calculations (Table 8). Two bands at 959 and 922 cm^{-1} in the spectrum of **6b** are assigned to the C–C ring deformation coupled with the =C–H and CH₂ rocking modes, respectively.

Our calculations predict a strong coupling of the Ge=C stretching vibration with the C–C ring deformation and the =C–H rocking mode, which results in two calculated values for each of the germadiene molecules, at 1196 cm^{-1} (Ge=C–C asymmetric stretch) and 843 cm^{-1} (Ge=C–C symmetric stretch) for **5b** (Table 4) and at 1216 cm^{-1} (Ge=C–C asymmetric stretch) and 830 cm^{-1} (Ge=C–C symmetric stretch) for **6b** (Table 5). Literature data predict the Ge=C stretch in H₂Ge=CH₂ to occur within the 785–904 cm^{-1} spectral region, depending on the level of calculations performed.²⁶ Recent RHF (DZ+d) calculations on Me₂Ge=CH₂ yielded a value of 844 cm^{-1} for the Ge=C stretching mode.²⁷ The π conjugation of the Ge=C bond with the C=C bond is expected to result in a noticeable shift to lower frequencies by analogy with the shift of the Si=C stretching frequency in going from 1-methyl-1-silene (989 cm^{-1})⁸ to **5a** (936 cm^{-1}) and **6a** (929 cm^{-1}). This gives reasonable support to the assignment of the observed bands at 834 cm^{-1} in **5b** and at 838 cm^{-1} in **6b** to the Ge=C stretching mode. In **5b-d₆** and **6b-d₆** a stronger coupling of this mode with several other modes is suggested by calculations (Tables 7 and 9) and makes the assignment to the Ge=C stretch less clear-cut. Therefore, we can only assume that the Ge=C stretch contributes significantly to the bands observed at 686 cm^{-1} in **5b-d₆** and 691 cm^{-1} in **6b-d₆** and to some bands at higher spectral frequencies that were not observed in our experiments due to their lower intensity.

An intense band at 787 cm^{-1} observed in the spectrum of **5b** is assigned on the basis of calculations (Table 4) to a mixed mode of several =C–H in-plane rocking motions. A corresponding band was not identified for **5b-d₆**, but in **6b-d₆** the =C–D in-plane bending mode was observed at 663 cm^{-1} , in accord with the calculations (Table 9).

The out-of-plane =C–H wagging modes were observed in **5b** at 682 cm^{-1} and at 778 cm^{-1} in **6b** as high-intensity bands in agreement with the calculations (657 and 769 cm^{-1} , respectively) and with the presence of this mode in siladienes^{5c} at 742 cm^{-1} in **5a** and at 790 cm^{-1} in **6a**. In **5b-d₆** the out-of-plane =C–D wagging mode is observed at 509 cm^{-1} , in agreement with the calculated value of 483 cm^{-1} (Table 8), whereas in **6b-d₆** this type of vibrational mode was found at 416 cm^{-1} .

We believe that the observed bands at 635 cm^{-1} in **5b** and at 698 cm^{-1} in **6b** belong to an out-of-plane CH₂

wagging mode coupled with the =C–H wagging mode, as predicted by calculations (Tables 4 and 5). In **6b-d₆** this mode is observed at 465 cm^{-1} , whereas in **5b-d₆** it contributes to a band at 509 cm^{-1} , already assigned earlier to the =C–D out-of-plane wagging mode. A band observed at 631 cm^{-1} in the spectrum of **6b** is assigned to the in-plane =Ge–H rocking mode, shifted to 454 cm^{-1} in **6b-d₆** in agreement with calculations (Tables 5 and 9). The same mode was not detected for **5b**, presumably because of its lower calculated IR intensity (Table 4).

The Ge–C stretch is calculated to appear at 586 cm^{-1} in **5b** and at 572 cm^{-1} in **6b** and to shift to 561 and 532 cm^{-1} in **5b-d₆** and **6b-d₆**, respectively. The only band matching these predicted values was observed for **6b-d₆** at 529 cm^{-1} . The remaining band at 621 cm^{-1} observed in the spectrum of **6b-d₆** is attributed to a twisting ring deformation, on the basis of calculations (Table 9).

Conclusion

The photochemical decomposition of diazidogermacyclopentene **4b** proceeds via a mechanism similar to that established earlier for the silicon analogue **4a** and results in the formation of germole **1b** along with the germylene **2b** as the most abundant products and of the germadienes **5b** and **6b** as minor products. Product structures were attributed on the basis of the response of the photochemical steady state to variations in irradiation wavelength, of the UV and IR spectra, including IR isotopic shifts in perdeuterated analogues, and of *ab initio* calculations of IR frequencies and intensities. It is proposed that the germole **1b** can be photochemically interconverted with the germadiene **5b**, the germylene **2b** with germadiene **6b**, and the two germadienes **5b** and **6b** with each other. In addition, there is either a minor photochemical path directly from **2b** to **1b**, or the photoconversion of **2b** to **6b** is followed by a hot ground state rearrangement of some of the **6b** into **1b**.

The calculations yielded planar optimized geometries for **1b**, **2b**, **5b**, and **6b**, with Ge=C bond lengths shorter than those calculated for unconjugated germenes. The IR results suggest that C=Ge–C=C and Ge=C–C=C π conjugation in the germacyclopentadienes **5b** and **6b** is somewhat weaker than C=Si–C=C and Si=C–C=C π conjugation in the silacyclopentadienes **5a** and **6a**. The UV spectra show a significant difference in the $\pi \rightarrow \pi^*$ transition energies in **5b** and **6b**, accounted for at the Hückel level by the reduced magnitude of the GeC resonance integral relative to CC.

Acknowledgment. The initial support of this work by the U. S. National Academy of Sciences through a Visiting Scholarship Grant for V.N.K. and further support by the U. S. National Science Foundation are greatly appreciated.

OM960372+